STEM CELLS AND DEVELOPMENT
Volume 24, Number 12, 2015

DOI: 10.1089/scd.2014.0497

Identification and Dynamic Regulation of Tight Junction Protein Expression in Human Neural Stem Cells

Andrea K. Watters,[1] Slava Rom,[1] Jeremy D. Hill,[1] Marie K. Dematatis,[1] Yu Zhou,[1] Steven F. Merkel,[1] Allison M. Andrews,[1] Jonathan Cena,[1] Raghava Potula,[1,2] Andrew Skuba,[3] Young-Jin Son,[3] Yuri Persidsky,[1,2] and Servio H. Ramirez[1–3]

Recent reports indicate that neural stem cells (NSCs) exist in a cluster-like formation in close proximity to cerebral microvessels. Similar appearing clusters can be seen ex vivo in NSC cultures termed neurospheres. It is known that this neurosphere configuration is important for preserving stemness and a proliferative state. How NSCs form neurospheres or neuroclusters remains largely undetermined. In this study, we show that primary human NSCs express the tight junction proteins (TJPs): zonula occludens-1 (ZO-1), occludin, claudin-1, -3, -5, and -12. The relative mRNA expression was measured by quantitative polymerase chain reaction, and protein expression was confirmed by flow cytometry and immunofluorescence microscopy. Our results show that downregulation of TJPs occurs as neuronal differentiation is induced, suggesting that control of TJPs may be tied to the neuronal differentiation program. Importantly, upon specific knockdown of the accessory TJP, ZO-1, undifferentiated NSCs showed decreased levels of key stem cell markers. Taken together, our results indicate that TJPs possibly aid in maintaining the intercellular configuration of NSCs and that reduction in TJP expression consequently affects the stemness status.

Introduction

Neurogenesis within the adult mammalian brain, first discovered by Altman and Das in 1965, is limited to two distinct regions: (1) the subventricular zone (SVZ) of the lateral ventricles and (2) the subgranular zone (SGZ) of the dentate gyrus in the hippocampus [1–4]. Neural stem cells (NSCs) populate these two zones alongside cerebral blood vessels ultimately creating unique vascular niches, where the interaction of the circulatory and nervous systems generate a specialized microenvironment that promotes the processes of neurogenesis (stem cell self-renewal, cellular proliferation, and terminal differentiation along either neuronal or glial lineages) [3,5].

Adult neurogenesis is a phenomenon whereby newborn neurons and glia integrate into the mature neural network of either the olfactory bulb or dentate gyrus, aiding in the functions of olfaction or learning and memory retention, respectively [5,6]. NSCs appear to be arranged in a cluster-like formation surrounding cerebral blood vessels, and this orientation is believed to facilitate the migration and subsequent differentiation of NSCs into fully functional neurons and glia [7]. One advantage of such a configuration is the continuous supply of oxygen, nutrients, and other molecules carried by the blood, as well as the necessary removal of metabolic waste through venous circulation [5]. Similarly, a cluster-like configuration, or neurosphere, is produced in vitro with NSCs derived from both adult and fetal mammalian tissues [8,9].

In a neurosphere, NSCs are capable of expanding for up to 200 days ex vivo [10,11]. These cells comprise the outer portion of the neurosphere, while the core consists of differentiating neural progenitor cells (NPCs) [12]. These two cell populations are embedded in a complex extracellular matrix (ECM) [12]. NSCs also express integrins and cadherins that function in ECM and cell to cell adhesion; however, a variety of adhesion/junction molecules are still uncharacterized in neurosphere cultures [12,13].

Tight junction proteins (TJPs) play an important role in all epithelia, connecting adjacent cells, and forming a continuous barrier to limit the penetration of peripheral elements; moreover, with respect to the blood–brain barrier (BBB), TJPs are paramount to its specialized anatomical and physiological function. Endothelial cells of the BBB create the vascular lumen coursing through the SVZ and SGZ stem cell niches. These brain microvascular endothelial cells (BMVECs) express unique TJPs that produce both a physical barrier through cell to cell contact and an electrical resistance that limits the paracellular diffusion of charged molecules from the blood to the central nervous system (CNS).

[1]Department of Pathology and Laboratory Medicine, [2]Center for Substance Abuse Research, and [3]Shriners Hospitals Pediatric Research Center, Temple University School of Medicine, Philadelphia, Pennsylvania.

The TJP complex is composed of transmembranous occludin, claudins, and junctional adhesion molecules that connect to the actin cytoskeleton through intermediary TJP accessory/anchoring proteins ZO-1, -2, and -3 [14–16]. TJ complexes are highly dynamic structures that respond quickly to intracellular signaling events and may experience rapid changes in the subcellular distribution of their composite proteins, as well as fluctuations in gene expression and various post-translational modifications [15,17,18]. Interestingly, the TJP accessory proteins, ZO-1 and ZO-2, interact with the C terminus domain of connexin 43 (Cx43). As a principle component of CNS gap junctions, Cx43 contains numerous protein-binding sites for cytoskeletal attachment and participates in modulating the function of neurovascular/astrocytic gap junctions (reviewed by Matsuuchi and Naus) [19,20].

Gap junctions regulate intracellular Ca^{2+} fluctuations between NSCs to coordinate calcium-dependent signal transduction throughout the stem cell syncytia [21,22]. Spontaneous Ca^{2+} signaling through gap junctions is a highly ordered transduction event in the SGZ and SVZ that is essential for NSC proliferation [23]. Functional gap junctions expressed by NSCs consist of two hemichannels, formed by either homo or heterohexamers of Cx43, have been implicated in regulating NSC adhesion to radial glial cells that aid in progenitor cell migration from the stem cell niche and into mature neural networks [19]. Cx43 is highly expressed by NSCs; however, as these cells depart upon differentiation, Cx43 expression and, subsequently, the intracellular communication through Cx43 in the stem cell niches begin to subside [20,24,25].

Notably, second messenger Ca^{2+} signaling is also important in TJP complex modification as well as the regulation of neurogenesis by coordinating NSC functions, such as proliferation, migration, and differentiation in the SVZ and SGZ [15,26,27]. To date, no reports have identified whether NSCs express TJPs, and therefore, the role that TJPs may have on calcium-induced NSC proliferation, migration, or differentiation and the contribution that TJPs may have on the maintenance of the neurosphere, cluster-like configuration in stem cell niches, remain as areas open to investigation.

In this study, we examined the expression of TJPs in NSC cultures and explored the possibility that these proteins participate in the cell to cell adhesion observed in neurospheres. Our findings show that NSCs highly express ZO-1, occludin, claudin-1, -3, and -5 mRNA while proliferating in a neurosphere. When neuronal differentiation was induced, the expression of these TJPs was markedly downregulated. Conversely, knocking down the expression of ZO-1 and disrupting the formation of TJP complexes in neurosphere culture lead to a concurrent loss of the stem cell marker, Nestin. These results highlight the possibility that TJP expression in stem cell cultures may participate in the physical adherence observed between cells as well as the potential these protein complexes may play in maintaining a proliferative, nondifferentiated state.

Materials and Methods

Cell culture

NSCs derived from NIH-approved H9 (WA09) human embryonic stem cells (from here on shortened to H9-NSCs) were maintained on CELLstart™ and grown in the StemPro® NSC serum free medium (SFM) at 37°C and 5.0% CO_2 (all purchased from Life Technologies). Cell cultures were maintained and expanded according to the supplier's instructions (Invitrogen). The medium was changed every 2–3 days. Cells were passaged using Accutase (Innovative Cell Technologies, Inc.) when cell growth reached a minimum of 85% confluence. Primary human fetal NSCs (from here on shortened to fetal NSCs or F-NSCs) were obtained from the Birth Defects Research Laboratory (University of Washington, Seattle, WA) in full compliance with the NIH ethical guidelines. Donor sex and maturation were specified; all donors were between 94 and 108 days.

The isolation procedure has been detailed previously [28] with slight modifications. Briefly, brain tissue was incubated in 0.25% trypsin diluted in Hank's balanced salt solution (HBSS) for 45 min. Tissue was transferred into 4°C heat-inactivated fetal bovine serum, triturated, and kept on ice for 2–3 min. HBSS (4°C) was added to the tissue and then centrifuged at 500*g* for 20 min. The pellet was resuspended in F-NSC complete media consisting of x-Vivo 15 (without phenol red and gentamicin; Lonza) supplemented with 10 μg of basic fibroblast growth factor (Life Technologies), 100 μg of epidermal growth factor (Life Technologies), 5 μg of leukemia inhibitory factor (EMD Millipore), 60 ng/mL of *N*-acetylcysteine (Sigma-Aldrich), 4 mL of neural survival factor-1 supplement (Lonza), 5 mL of 100× N-2 supplement (Life Technologies), 100 U of penicillin, 100 μg/mL of streptomycin (Life Technologies), and 2.5 μg/mL of fungizone (Life Technologies). The tissue was mechanically dissociated with small-bore glass pipettes. Supernatants were filtered through a 40-μm cell strainer (Corning Life Science). Single-cell suspension was seeded at a minimum density of 20 million cells in a total 25 mL of complete media. Cells were passaged using Accutase when neurospheres grew to greater than 15 cells in diameter. Neurospheres larger than 40 μm in diameter were incubated in Accutase for 10 min. After mechanically dissociating the cells, 10 mL of F-NSC medium was added to stop trypsinization. The cell pellet was collected at 900 rpm for 5 min, resuspended in a fresh medium, and transferred to a new flask.

Directed differentiation

After one day of adherent culture, media was replaced with the Neural Differentiation Medium consisting of 1× Neurobasal Medium, 2% B-27 serum-free supplement, and 2 mM GlutaMAX-I supplement (all from Invitrogen) and supplemented with human recombinant brain-derived neurotrophic factor (BDNF) (10 ng/mL; Peprotech). H9- and F-NSCs were maintained on CELLstart. The differentiation medium was changed every 3–4 days.

Real-time quantitative polymerase chain reaction

The mRNA gene expression profile of TJPs and stem cell markers was established for both undifferentiated and differentiating fetal and H9-NSCs. RNA was isolated with the RNAqueous PCR kit (Ambion), and RNA purity and concentration were determined with a NanoDrop ND-1000 spectrophotometer (Thermo Fisher Scientific, Waltham, MA). cDNA conversion was performed by reverse transcription using the High-Capacity cDNA Reverse Transcription Kit (ABI). The cDNA (diluted 1:4) template was then mixed with both the TaqMan Universal PCR Master Mix

(ABI) and the corresponding human TaqMan Gene Expression Assay: *Nestin*: Hs04187831_g1, *Sox2*: Hs01053049_s1, *CLDN1*: Hs01076359_m1, *CLDN3*: Hs00265816_s1, *CLDN5*: Hs01561351_m1, *CLDN12*: Hs00273258_s1, *OCLN*: Hs001701 62_m1, *TJP1*: Hs01551876_m1, and *TJP2*: Hs00910541_m1 from ABI, according to the manufacturer's instructions; for internal controls, the human TaqMan gene expression predeveloped assays for *GAPDH* and *RPLPO* (Applied Biosystems) were also used. Quantitative polymerase chain reaction (qPCR) was performed on an Applied Biosystems StepOnePlus Real-Time PCR System. Raw data were analyzed with DataAssist software (Applied Biosystems) using the ΔΔCt method (relative quantification). Results are expressed in relative gene expression levels (fold) compared to the first group (cell line control) shown on the figure graphs.

Immunofluorescence staining and image analysis

TJP expression was evaluated on F-NSCs adhered to MilliEZ chamber slides (Millipore) coated with Poly-D-Lysine (50 μg/mL; Sigma) and on H9-NSCs adhered to MilliEZ chamber slides coated with CELLstart. Cells were fixed with 3% formaldehyde and permeabilized with 0.05% Triton X-100 (Sigma-Aldrich) in 1× phosphate-buffered saline (PBS; Invitrogen). Primary monoclonal antibodies to Nestin (10C2) (diluted 1:100; Abcam), claudin-5 (EPR7583) (1:50; Abcam), and Sox2 (O30-678) conjugated with Alexa Fluor 488 (diluted 1:200; BD Biosciences) and polyclonal antibodies to ZO-1, occludin, claudin-1, claudin-3 (all diluted 1:50; Invitrogen), and Nestin (1:200; Abcam) were diluted in a blocking solution consisting of 3% bovine serum albumin (BSA; Sigma-Aldrich) + 0.1% Triton X-100 in PBS and incubated with NSCs overnight at 4°C. Differentiating NSCs were also stained with a primary monoclonal antibody (TU-20) to neuron-specific class III β-Tubulin (1:500; Abcam). Cells were rinsed, and secondary antibodies conjugated to Alexa Fluor 488 and Alexa Fluor 594 (diluted 1:200; Invitrogen) were added for 1 h. The slides were mounted with a ProLong antifade reagent containing DAPI (Invitrogen). Imaging was performed using a CoolSNAP EZ CCD camera (Photometrics) coupled to a Nikon i80 Eclipse (Nikon). For neurosphere imaging, a Leica TCS SP5 II MP multiphoton microscope (Leica Microsystems) configured with a tunable femtosecond pulsed Mai Tai Ti:Sapphire laser (Spectra Physics) with a resonant scanner and non-descanned detector or NDD detectors. The cells were observed with a 20× dipping objective (NA 0.95) and images were acquired using Leica's LAS imaging software.

Flow cytometry

TJPs in H9- and fetal NSCs were measured by flow cytometry. Sample sizes of 1×10^6 H9- and F-NSCs were collected using EDTA (3 mM; Invitrogen). NSCs were fixed and stored at 4°C until labeling in a fixation buffer (eBiosciences). Cells were placed in a permeabilization buffer (eBiosciences), containing primary antibodies to TJPs, ZO-1, occludin, claudin-1, claudin-3, and claudin-5, and stem cell markers, Sox2 and Nestin, for 30 min. Differentiating NSCs were also stained with a primary polyclonal antibody to human microtubule-associated protein 2 (Map2; US Biological) or monoclonal antibody (TUJ1) to class III β-Tubulin conjugated with Alexa Fluor 647 (BD Biosciences). After the cells were rinsed with a permeabilization buffer, secondary antibodies conjugated to either FITC or APC were added for 30 min. Unless otherwise specified, the same antibodies and dilutions were used as in the Immunofluorescence Staining and Image Analysis section. Cells were rinsed and resuspended in a flow buffer consisting of 1% BSA in 1× PBS. Acquisition and analysis of the labeled cells were then performed using a FACS Calibur of FACS-Canto II flow cytometers (BD Biosciences). Acquisition parameters and gating were controlled by CellQuest software (BD Biosciences). Data analysis was performed with FlowJo software (FlowJo, LLC). The data represent the fluorescence intensity of gated populations (as determined by isotype-matched controls) of at least 10,000 events recorded in a single experiment that was repeated thrice.

Transient transfection

Transfection into H9-NSCs was performed by electroporation using one pulse of 1,100 V and 30 ms with the Neon® transfection system (Life Technologies) according to the manufacturer's instructions. The use of the Neon transfection system on H9-NSCs allows for 30%–60% transfection efficiency. The concentration of ON-TARGETplus SMARTpool siRNA for *TJP1* (ZO-1), and of ON-TARGETplus nontargeting pool was 50 nM and of the siGLO green transfection indicator was 50 nM (all purchased from Thermo Scientific). Cells were immediately grown on CELLstart in the StemPro NSC SFM complete medium at 37°C and 5.0% CO_2. After 48 h, cells were collected using EDTA. Cells were stained with antibodies against ZO-1 and Nestin. Acquisition and analysis of the labeled cells were then performed using a FACS-Canto II flow cytometer (BD Biosciences) and analyzed with FlowJo software (Tree Star, Inc.). The H9 population lying within the FITC-positive gate was analyzed. The data represent at least 10,000 events collected per experiment.

Statistical analysis

The values shown in all figures and those mentioned in the text represent the average ± SEM of experiments that were conducted multiple times (as indicated). Statistical significance ($P < 0.05$) was determined by performing unpaired two-tailed Student's *t*-test or through multiple group comparisons performed by ANOVA with Dunnett's post hoc test utilizing Prism v5 software (GraphPad Software, Inc.).

Results

Gene expression profile for proteins associated with the formation of tight junction complexes

We evaluated NSCs derived from H9 (WA09) human embryonic stem cells (H9-NSCs) (Fig. 1A) and those isolated from human fetal brain tissue (F-NSCs) (Fig. 1B). H9-NSCs were grown in adherent culture as a monolayer, while F-NSCs were grown in suspension as neurospheres. The expression profile of TJPs was evaluated by real-time qPCR. First, NSC cellular markers, Nestin and Sox2, were evaluated. As shown in Fig. 1C, both cellular markers are expressed. Established from a histiocytic lymphoma, U937 cells have a monocytic phenotype [29] and express very

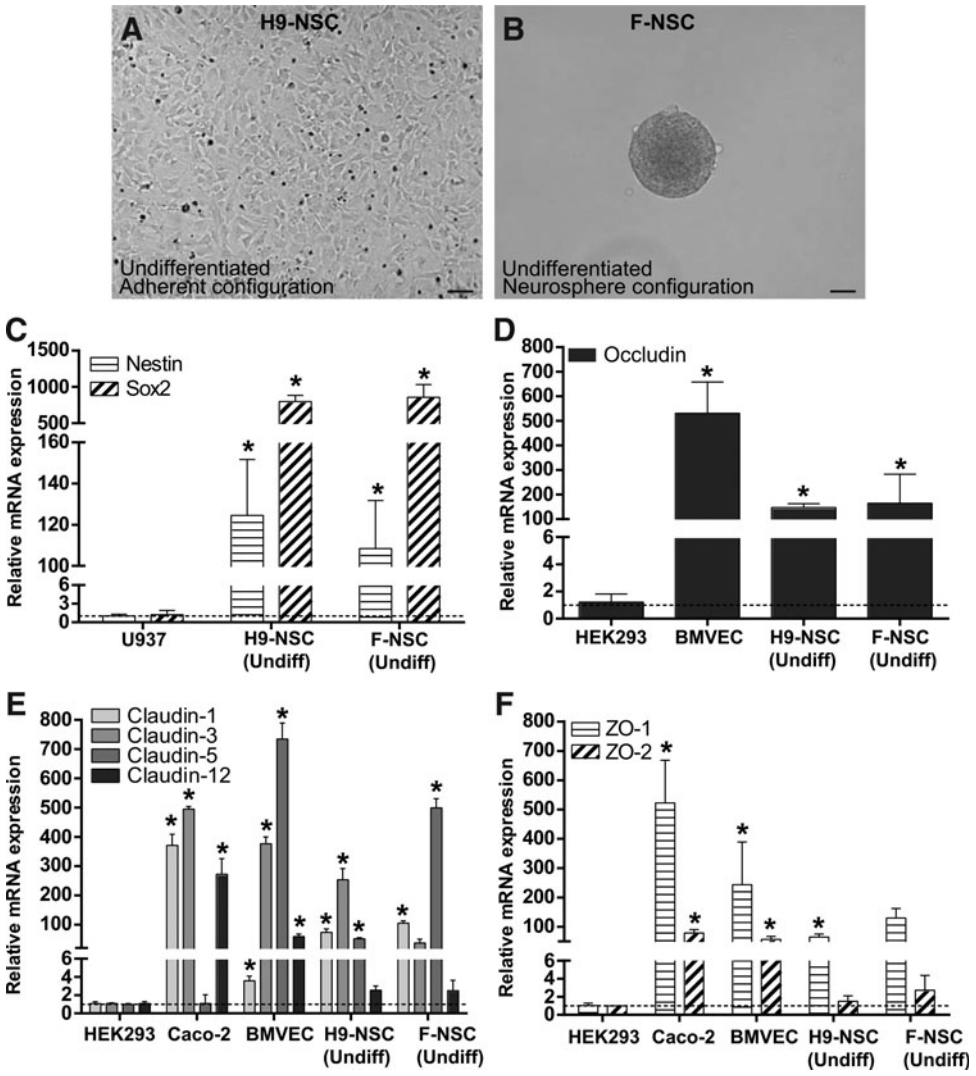

FIG. 1. Polymerase chain reaction (PCR) data shows relative mRNA expression of tight junction proteins (TJPs) in H9 and fetal neural stem cells (F-NSCs). **(A)** Representative image of H9-NSCs in the undifferentiated state in adherent culture. **(B)** Representative image of F-NSCs in the undifferentiated state in neurosphere configuration. **(A, B)** are shown at 20× magnification with a scale bar set at 100 μm. **(C)** Relative mRNA expression of NSC markers Sox2 and Nestin in U937 cells and in primary NSCs. **(D)** Relative mRNA expression of occludin in HEK293 cells, brain microvascular endothelial cells (BMVECs), and NSCs. **(E)** Relative mRNA expression of claudin-1, -3, -5, and -12 in HEK293 cells, Caco-2 cells, BVMECs, and NSCs. **(F)** Relative mRNA expression of ZO-1 and ZO-2 in HEK293 cells, Caco-2 cells, BVMECs, and NSCs. The results are expressed as the average fold change ± SEM in gene expression compared to the first group shown in the graph. In all comparisons, U937, HEK293, BMVEC, and Caco-2 cells were used as controls for the indicated gene expression target. The *asterisk* indicates statistical significance ($P < 0.001$).

little mRNA for Nestin and Sox2. Therefore, U937 cells were used to derive the relative expression levels of both NSC markers in H9-NSCs and F-NSCs. Interestingly, even though H9-NSCs were cultured as adherent cells compared to the neurospheres in F-NSCs, the high level of mRNA expression of Sox2 and Nestin was similar in both cell types with a roughly 116-fold increase in Sox2 and 1,000-fold increase in Nestin (Fig. 1C).

For the assessment of gene expression for TJPs, studies were focused on occludin, barrier (or strand)-forming claudins known to have brain tissue distribution such as claudin-1, -3, -5, -12, and the scaffold proteins, ZO-1 and ZO-2 [30,31]. The human embryonic kidney cell-line HEK293 cells do not form tight junctions, (TJ), but do express low levels of mRNA for TJPs, which is likely highly unstable and degrades before making it to the protein [32]. However, for the purpose of comparison, HEK293 cells were used to calculate the relative expression of genes coding for TJPs in NSCs (Fig. 1D–F). Primary human BMVECs were used as a control since these cells highly express TJPs [33]. Expression of occludin mRNA in NSCs was high with an ∼150-fold increase in both H9 and F-NSCs over control (Fig. 1D). As expected, BMVEC mRNA expression for occludin was very high with a 550-fold increase. Caco-2 cells are an intestinal epithelial cell line, which expresses TJPs, although of a different proteomic configuration than the brain endothelial cell. Membrane fractions of Caco-2 cells show claudin-1, claudin-3, and claudin-12 expression, but no claudin-5 expression [34,35]. Meanwhile, BMVECs predominantly express claudin-3 and claudin-5 [15]. Of the TJ-expressing cell lines, Caco-2 cells expressed the highest level of mRNA for claudin-1 with a 400-fold increase and BMVECs the lowest level with a 4-fold increase.

H9 and F-NSCs showed a moderately high expression of mRNA for claudin-1 with roughly a 150-fold increase in both cell types. Claudin-3 mRNA expression was high for Caco-2 cells and BMVECs with a 500- and 400-fold increase, respectively. In comparison, NSCs had less, but still significant claudin-3 expression. The fold increase for H9-NSCs was three times greater compared with F-NSCs. There was marginal mRNA expression for claudin-5 in Caco-2 cells. Claudin-5 mRNA expression in H9-NSCs and F-NSCs was considerably high with a 250- and 600-fold increase when compared to the 800-fold increase in BMVECs. Claudin-12 mRNA expression was high in Caco-2 cells with

a 300-fold increase, moderate in BMVECs with a 100-fold increase, and very low in NSCs with a 3-fold increase in both H9 and fetal types (Fig. 1E).

Next, the scaffold proteins ZO-1 and ZO-2, critical for assembly of the TJ complex, were analyzed. Previous reports have shown that Caco-2 cells express both ZO-1 and ZO-2 proteins [36]. ZO-1 mRNA expression was high in Caco-2 cells with a 500-fold increase. mRNA expression in NSCs was comparable to that of BMVECs. A 250-fold increase in BMVECs was observed compared to a 150-fold increase in F-NSCs and 100-fold increase in H9-NSCs. In general, there was less mRNA expression for ZO-2 than for ZO-1 in all TJ-expressing cell types. The mRNA expression for ZO-2 was moderate for Caco-2 cells and BMVECs with a roughly 100-fold increase for both cell types. Interestingly, there was very low ZO-2 mRNA expression for NSCs with only roughly a 3-fold increase over the HEK293 control for both types of NSCs (Fig. 1F). These data confirm that NSCs express TJ mRNA in a manner consistent with cells known to have high levels of TJ mRNA expression.

Detection of TJP expression through FACS

To investigate whether TJP mRNA expression in NSCs correlated with their protein expression, analysis by FACS was performed. First, antibodies against common NSC markers were used. As shown in Fig. 2B, ~93% of the H9-NSC population was positive for stem cell markers, Sox2 and Nestin (Fig. 2B), indicating that proliferating NSCs in culture maintained their stemness state. Next, TJP immunostaining was counterstained with stem cell marker Sox2 to identify the presence and the percent of the population expressing the TJP. Of the Sox2-positive population, ~91% of the cells were positive for ZO-1, 89% for occludin, 42% for claudin-1, 91% for claudin-3, and 85% for claudin-5 (Fig. 2C–F).

Likewise, F-NSCs expressed Sox2 and Nestin. In regard to F- NSCs, similar expression profiles as H9-NSCs were observed, although Sox2 was lower in F-NSCs when compared to H9-NSCs (data not shown). Overall, in all isolations of F-NSCs greater than 97% of the cells expressed, occludin, ZO-1, claudin-3, and claudin-5 with 32% of the cells expressing claudin-1 (data not shown). FACS analysis confirms that NSCs express transmembrane TJPs and that their expression correlates with NSC markers, Sox2 and Nestin.

Cellular distribution of TJPs in NSCs

To characterize TJP cellular distribution, visualization by indirect immunofluorescence and microscopy was performed. First, undifferentiated and proliferating NSCs were evaluated for the presence of NSC markers, Sox2 and Nestin. Double-immunostaining with anti-Nestin and anti-Sox2 antibodies showed strong immunoreactivity of the two targets in H9 and F-NSCs, Figs. 3A–C and 4A–C, respectively. Interestingly, Sox2, a transcription factor for maintaining pluripotency, was found to be primarily in the nuclear compartment for H9-NSCs and more cytosolic for F-NSC (Figs. 3B and 4B). Nestin, an intermediate filament

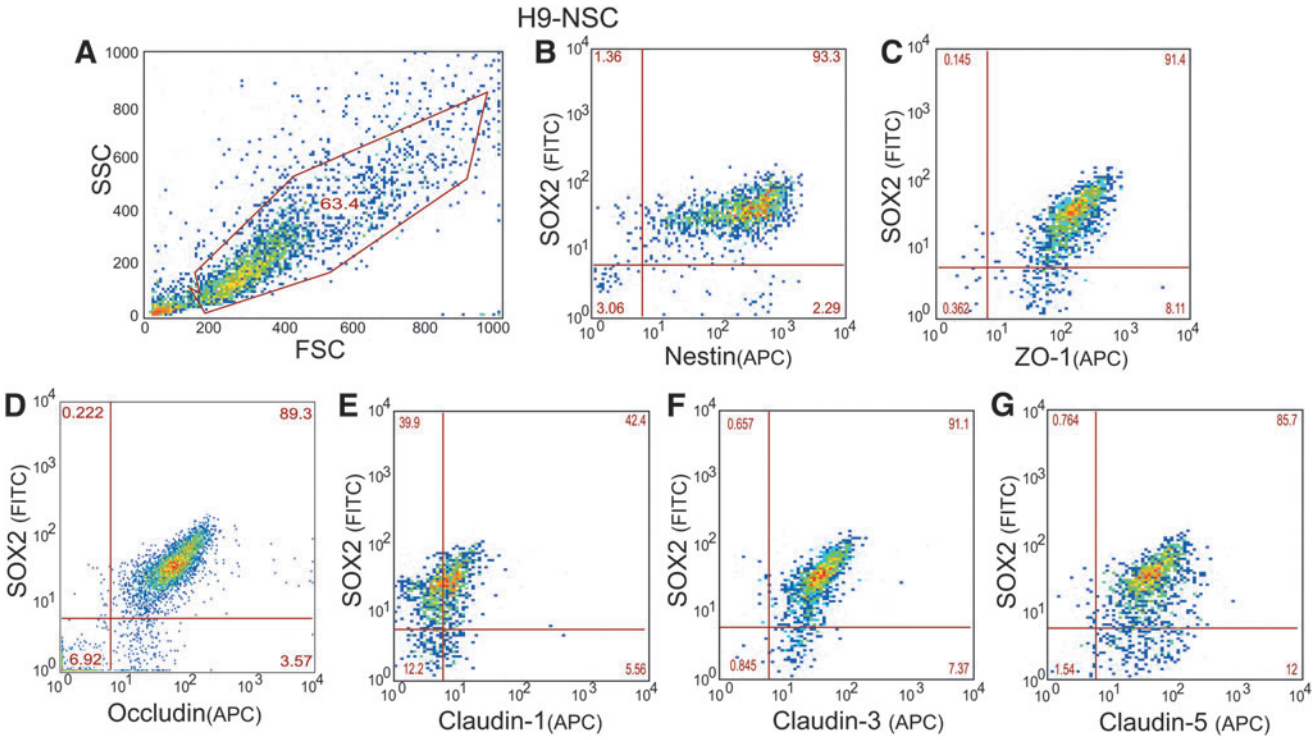

FIG. 2. Representative plots of FACS analyses of TJPs on H9-NSCs. **(A)** Demonstrates typical gating parameters for subsequent study of H9-NSC populations. Analyses were based upon 10,000 cell counts within the gate. **(B)** H9-NSCs were immunostained for Nestin and Sox2 to confirm NSC phenotype. Sox2 expressing H9-NSCs were colabeled for TJPs ZO-1 **(C)**, occludin **(D)**, claudin-1 **(E)**, claudin-3 **(F)**, and claudin-5 **(G)**. Number in the *quadrants* of each plot indicates the percentage of cells showing no expression of the target (*bottom left quadrant*), Sox2 only (*upper left quadrant*), the specific TJPs (*bottom right quadrant*), or both Sox2 and the particular TJP (*upper right quadrant*).

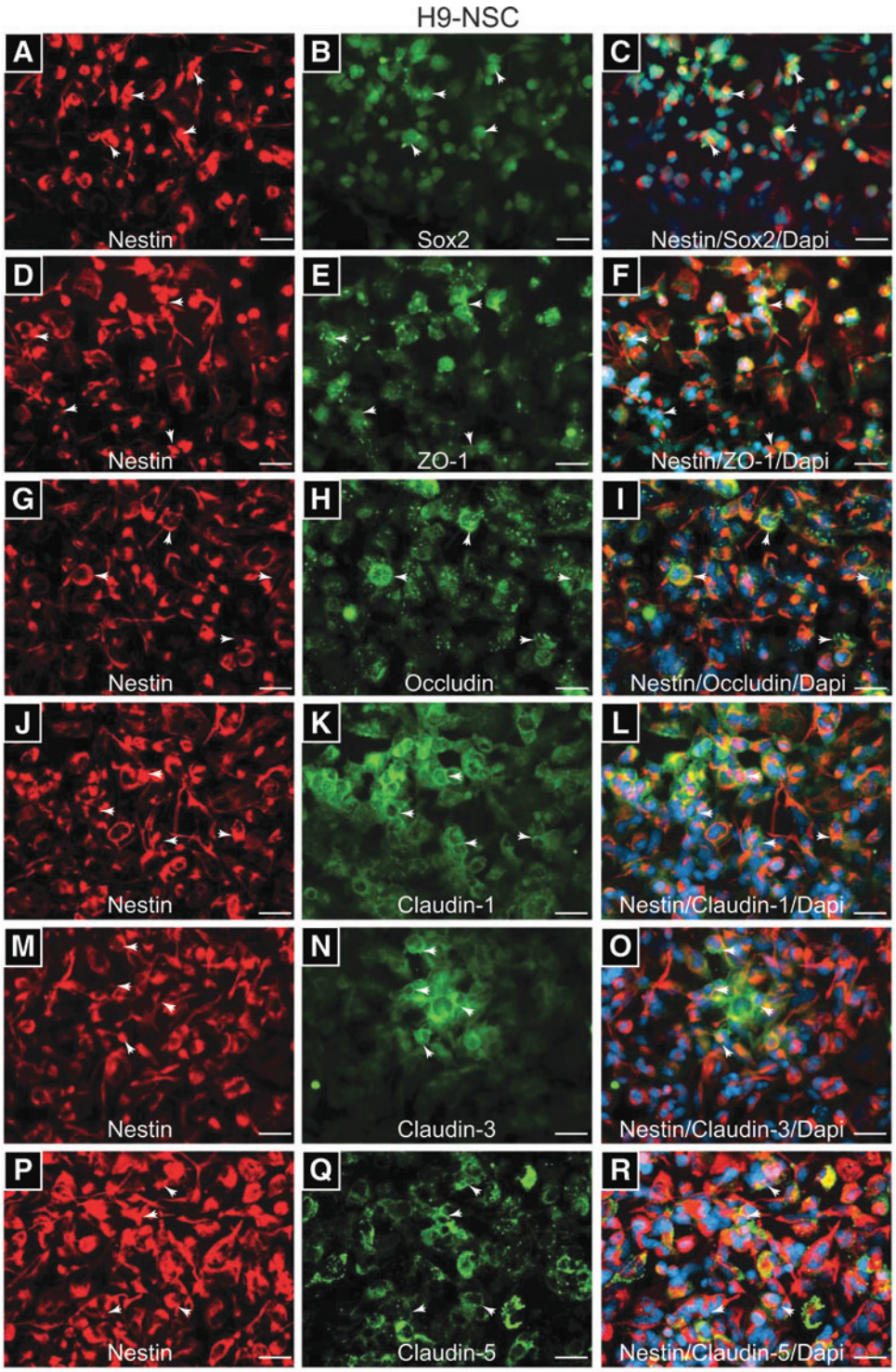

FIG. 3. Distribution of TJPs on H9-NSCs. **(A** and **B)** Shows immunopositive F-NSCs with anti-Nestin and anti-Sox2 antibodies, confirming the NSC phenotype. H9-NSCs immunopositive for ZO-1 **(E)**, occludin **(H)**, claudin-1 **(K)**, claudin-3 **(N)**, and claudin-5 **(Q)**. The *first column* **(A, D, G, J, M,** and **P)** shows the same neurosphere (s) as the *middle column* is also immunopositive for the stem cell marker Nestin. The images on the *right column* **(C, F, I, L, O,** and **R)** show the preceding two images merged along with the nuclear counterstain DAPI. All images are shown at 40× objective power with scale bars at 20 μm. *Arrows* indicate areas where the expression appears intercellular.

protein, appeared cytosolic and distinctly fiber like for H9 and fetal NSCs (Figs. 3A, D, G, J, M, P and 4A, D, G, J, M, P). ZO-1, the anchor protein necessary for TJ assembly [15,31], appeared distributed throughout the cytoplasm and membranous areas of H9–NSCs, but was more concentrated at the cellular membranes for F-NSCs (Figs. 3E and 4E). Occludin and claudins are transmembrane proteins that directly bind to specific sites on ZO-1 [37]. Occludin (Figs. 3H and 4H) and claudin-1 (Figs. 3K and 4K) were observed at intercellular areas for both H9 and F-NSCs. Furthermore, when compared to the other TJPs, claudin-1 expression appeared the most distinctively membranous and concentrated at intercellular areas when compared to the other claudins. Claudin-3 appeared cytosolic and filamentous-like in F-NSCs, with only a few cells showing great intensity at intercellular regions (Fig. 4N). Claudin-3 appeared mainly cytosolic, although in cells with high expression it appeared to be concentrated with high intensity at cell–cell junctions in H9-NSCs (Fig. 3N).

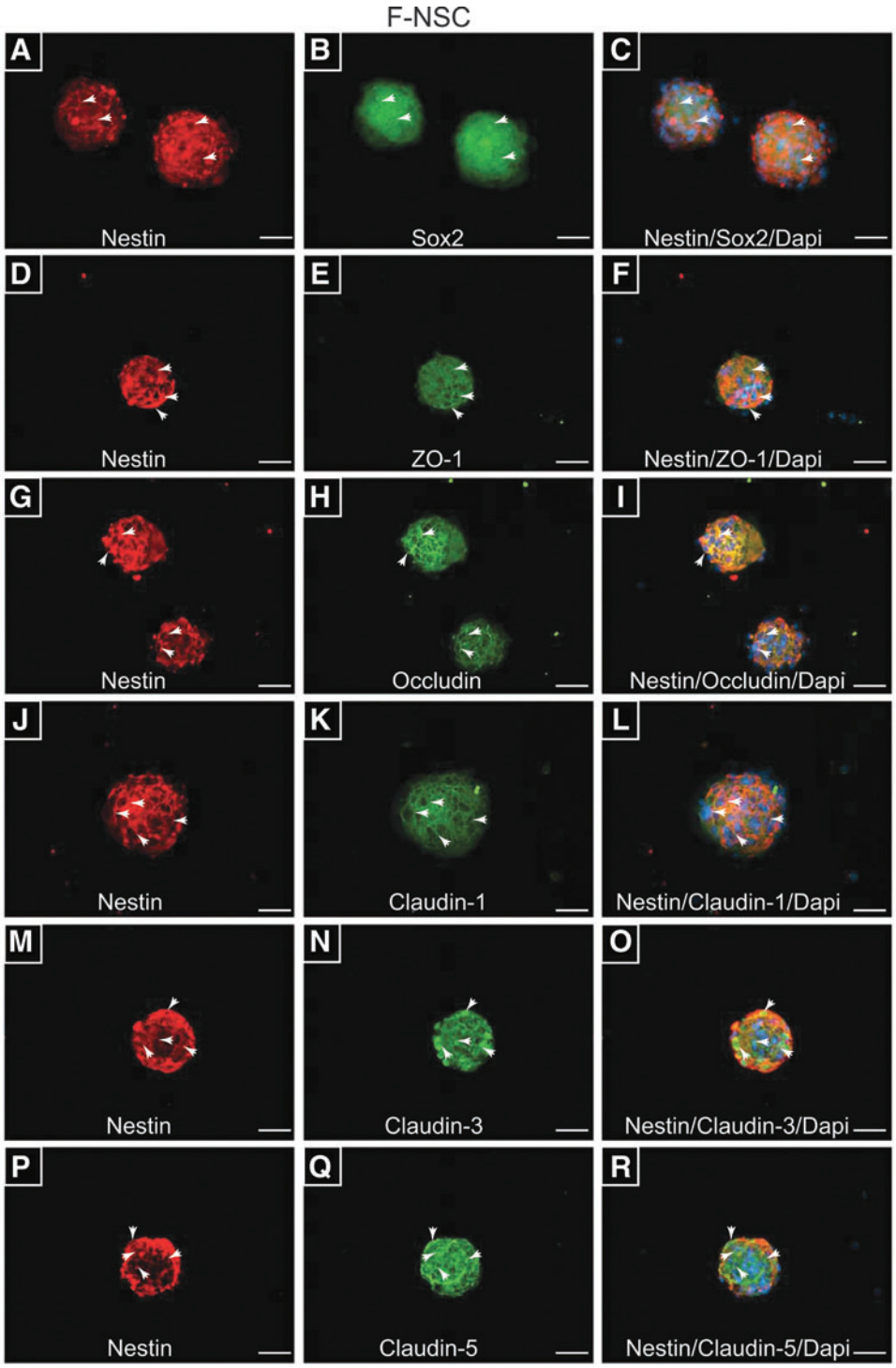

FIG. 4. Distribution of TJPs on F-NSCs. **(A** and **B)** Expanded cultures of F-NSCs neurospheres show immunopositive reactivity with antibodies to stem cell markers Nestin and Sox2, respectably. **(D, G, J, M,** and **P)** Nestin-positive neurospheres also appear immunopositive for TJPs: ZO-1 **(E)**, occludin **(H)**, claudin-1 **(K)**, claudin-3 **(N)**, and claudin-5 **(Q)**. Note the transmembrane and/or cytosolic localization of TJPs, while Nestin appears cytosolic and filamentous. The images on the *right column* **(C, F, I, L, O,** and **R)** show the preceding two images merged along with the nuclear counterstain DAPI. All images are shown at 40× objective power with scale bars at 20 μm. *Arrows* indicate areas where the expression appears intercellular.

Interestingly, the intensity of claudin-3 was much greater for F-NSCs even though the relative mRNA expression was three times less compared with H9-NSCs. Claudin-5 was highly concentrated at intercellular areas, but also throughout the cytoplasm in H9 and F-NSCs (Figs. 3Q and 4Q). Of note, for better visualization of morphological patterns of occludin and ZO-1 in H9-NSCs, high-magnification images (at 60× and 100× oil-objective magnification) are provided in Supplementary Fig. S1; supplementary materials are available online at http://www.liebertpub.com/scd. Together, these data suggest that NSC TJPs are distributed along the cellular membrane and concentrated at intercellular areas representing a fully functional TJ complex.

The expression of TJPs in NSCs suggests the likely assembly of intercellular tight junction complexes between adjacent cells. Measurement of resistance by Electric Cell-substrate Impedance Sensing or ECIS® was performed as a means to analytically evaluate the tightness of H9-NSC monolayers. Therefore, using the ECIS Z-theta 96-well array station from Applied Biophysics, H9-NSCs were seeded

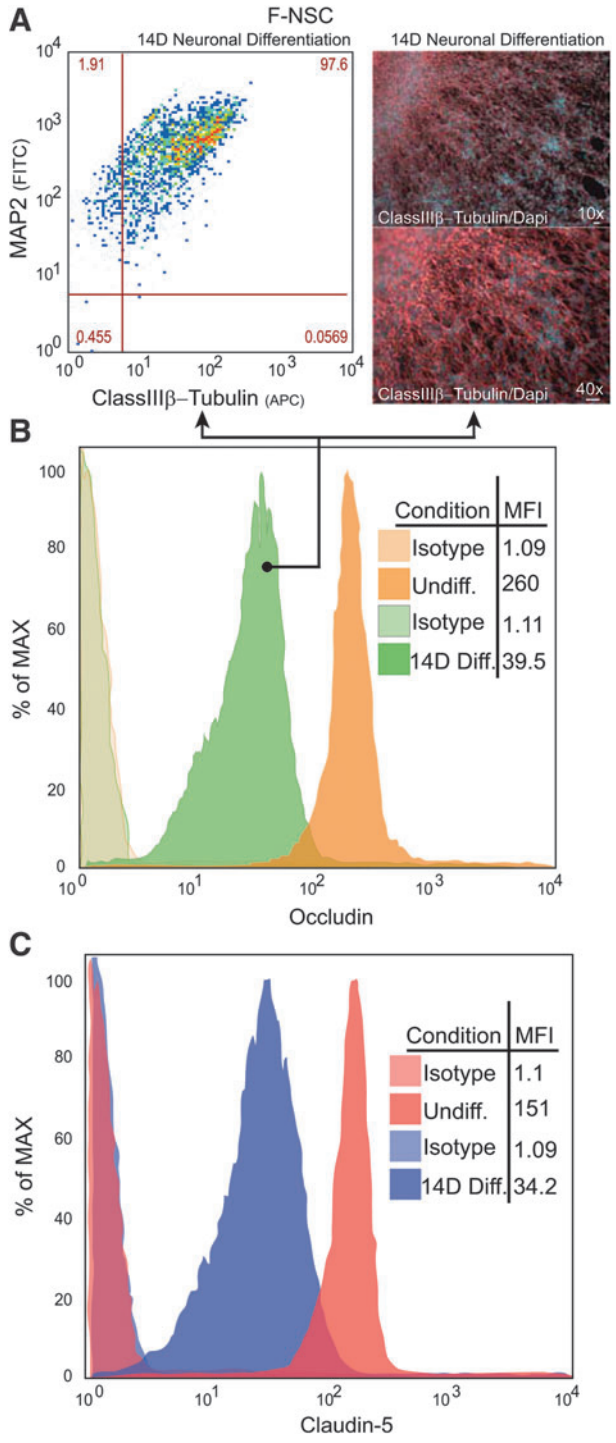

FIG. 5. Downregulation of TJP expression in differentiated F-NSCs. Neurospheres were induced to differentiate toward a neuronal phenotype for 14 days. **(A)** FACS analysis of differentiated F-NSCs upregulate neuronal markers and double positive for Map2 and class III β-Tubulin. Representative images (on the *right*) demonstrate the typical morphological changes of F-NSCs differentiating neurons that are observed migrating out of the neurosphere. FACS histograms for occludin **(B)** and claudin-5 **(C)** expression in undifferentiated and differentiated F-NSCs. Note, in differentiated neurospheres, the expression of TJP decreases; the mean fluorescence intensity (MFI) (expressed in percent of the maximum intensity) is indicated within the graphs.

on top of microelectrodes and allowed to grow. Input of a low-frequency current is impeded in a manner related to cell attachment and configuration. The low AC frequency used follows the path of least resistance, particularly between adjacent cells (i.e, paracellularly).

To compare the relative intercellular tightness between adjacent cells, the resistance was measured on monolayers of H9-NSCs and compared to those generated by brain endothelial cells and HEK293 cells (Supplementary Fig. S2). BMVECs, which are barrier forming due to the presence of tight junctions, had the highest resistance measurements (in ohms) followed by H9-NSCs and finally HEK293 cells (which form adherent junctions, but have no tight junctions). At 24 h, normalization to the values produced by HEK293 cells provided the following results (average fold ± SD): HEK293 = 1.0 ± 0.106, BMVEC = 30.560 ± 1.992, and H9-NSC = 7.143 ± 0.533. These analyses show that H9-NSCs generate a resistance that is seven times higher than that measured for HEK293 cells. Together, these results give credence to the notion that membrane localization of TJPs in NSCs is likely involved in forming intercellular tight junction complexes.

Neuronal differentiation of NSCs affects TJP expression

H9 and F-NSCs were grown in adherent culture and supplemented with the neurobasal medium with BDNF for 14 days; 97% of the F-NSC population was double positive for neuronal markers, Map2 and class III β-Tubulin, confirming that neuronal differentiation was induced (Fig. 5A). Immunofluorescence staining and imaging showed typical neuronal morphological changes with intense class III β-Tubulin protein expression (Fig. 5A). Similar differentiation outcomes were obtained for differentiated H9-NSCs (data not shown).

As seen earlier, FACS analysis indicated that over 98% of the NSCs expressed ZO-1, occludin, and claudin-5. FACS (histograms) mean fluorescence intensity (MFI) determinations showed that occludin (Fig. 5B) and claudin-5 (Fig. 5C) expression was decreased at 14 days of neuronal-induced differentiation when compared to undifferentiated NSCs. Typical results showed that the MFI for occludin decreased from 260 ± 30 to 39 ± 5, while MFI of claudin-5 decreased from 151 ± 22 to 34 ± 8 indicating approximately a 6.6- and 4.4-fold downregulation for occludin and claudin-5, respectively.

H9-NSCs showed a similar downregulation in TJPs during differentiation (data not shown). Ninety-eight percent of the H9-NSCs were double positive for Map2 and class III β-Tubulin upon differentiation. Over 93% of the H9 population expressed ZO-1, occludin, or claudin-5. The MFI of occludin decreased by 3.6-fold from 556 ± 51 to 153 ± 19 post-14-day differentiation. The MFI of claudin-5 decreased from 416 ± 72 at the undifferentiated state to 62 ± 7 at 14-day differentiation; a decrease of 6.7-fold. Analysis of the gene expression for the TJPs after 14-day neuronal differentiation also showed downregulation (Fig. 6), indicating regulation of protein expression at the transcriptional level rather than protein turnover.

Compared to levels in the undifferentiated cells, the following (average) percent of mRNA downregulation was observed in H9-NSCs: 70% for ZO-1, 30% for ZO-2, 82% for occludin, 20% for claudin-1, 60% for claudin-3, 40% for

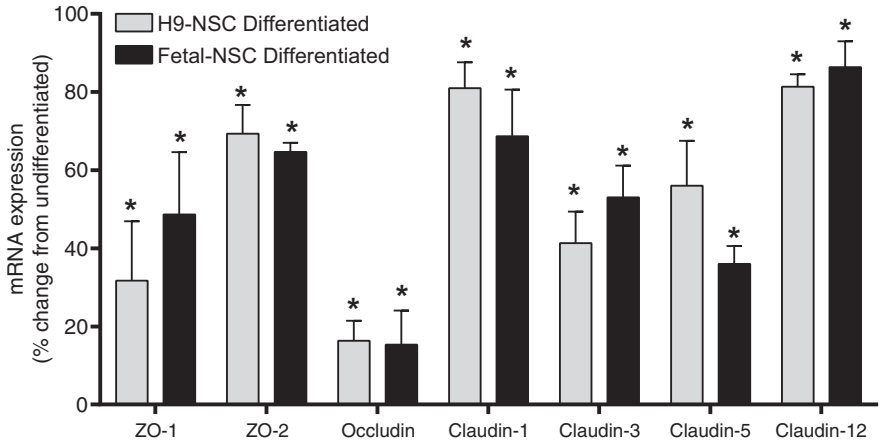

FIG. 6. Decreased expression of TJPs in differentiated H9-NSCs and F-NSC. Comparative mRNA expression analysis by quantitative polymerase chain reaction of genes coding for TJPs. The results show the mean ± SEM of the percent change from the levels found in the corresponding undifferentiated state. The *asterisk* indicates statistical significance ($P < 0.001$).

claudin-5, and 20% for claudin-12. F-NSCs had similar trends as H9-NSCs, although with slight differences in gene regulation. The results for F-NSCs compared to the undifferentiated were as follows: 50% for ZO-1, 35% for ZO-2, 82% for occludin, 30% for claudin-1, 50% for claudin-3, 60% for claudin-5, and 15% for claudin-12. Together, these results suggest that NSCs greatly downregulate TJP expression as a function of differentiation.

Targeted downregulation of ZO-1 in undifferentiated NSCs induces loss of stem cell markers

The TJP ZO-1 is necessary to nucleate the TJ complex serving as a scaffold to anchor occludin and claudins and forming a bridge to the cytoskeleton [37]. We hypothesized that by knocking down ZO-1, TJ would be compromised and trigger NSCs to lose their stemness. To test this premise, H9-NSCs were transfected with a targeting siRNA pool for ZO-1 along with a nontargeted FITC-labeled siRNA control. As can be seen in Fig. 7A, the nontargeted FITC-labeled siRNA showed approximately a 31% transfection efficiency, serving also as the means to gate for the population transfected. Transfection of the nontargeted siRNA had no effect on ZO-1 expression (Fig. 7B). However, transfection of the targeted siRNA for ZO-1 (along with the nontargeted FITC labeled) showed a decrease in both the possible cell populations expressing ZO-1 and Nestin (Fig. 7C).

Typical results after 48 h showed a decrease of 24% downregulation in Nestin, from 70.4% to 54.2% positive cells. A 38% downregulation in Sox2 was also observed, from 47.4% to 29.7% positive cells. For ZO-1-Nestin double-positive cell populations, a 36.4% decrease was observed, from 93.6% to 57.2% positive cells. siRNA-mediated knockdown of ZO-1 also induced a 41% decrease in ZO-1-Sox2, from 56.7% to 33.6% positive cells. Although transfection efficiencies were overall much lower for F-NSCs, the loss of Nestin and Sox2 after siRNA specific to ZO-1 transfection was also observed (data not shown). These results point to a possible mechanism in which the TJP scaffold, ZO-1, may be downregulated to promote NSC loss of stemness and induction of differentiation.

Discussion

In the brain, TJ are present throughout the vasculature and at the choroid plexus (CP). TJPs present between endothelial cells form the basis of the physical barrier associated with the BBB and those at CP epithelial cells forms the blood-cerebrospinal-fluid barrier [38]. The predominant TJPs expressed in the brain include occludin, claudin-1, -3, -5, -12 and ZO-1 and -2 [39]. The TJ complex responds quickly to intracellular signaling changes and shows rapid changes in expression, subcellular redistribution, and post-translational modifications [15,17,18].

NSCs in the brain exist in a neurocluster-like configuration found in close proximity at bifurcating cerebral microvessels of the SVZ and SGZ [3]. A similar configuration is found when primary NSCs are cultured in vitro. These cells have the characteristic free-floating three-dimensional cluster-like formation, and the cells maintain their proliferative state, self-renewal, and multipotency. It is known that this neurosphere configuration or stem cell to cell contact is important for preserving stemness and a proliferative state. How NSCs form neurospheres or neuroclusters remains largely unknown. Particularly, this study was designed to answer the question of whether or not TJPs could be detected in NSC cultures. To answer this question, the studies presented in this report utilized both primary human fetal NSCs obtained from the Birth Defects Research Laboratory at the University of Washington and a primary NSC line derived from H9 (WA09) human embryonic stem cells.

Primary human fetal NSCs formed free-floating neurospheres in culture, while the H9-NSCs were cultured as adherent monolayers. Part of the reasoning to use these two types of cells was to determine whether differences existed between the type of TJPs found in cell to cell interactions between monolayer versus neurosphere-grown NSC cultures.

Analysis first centered on profiling the mRNA and protein expression of barrier-forming TJPs in NSCs. To ensure proper culturing conditions, the NSC marker was confirmed as having $Sox2^{hi}$ and positive for Nestin [40] (Fig. 1). TJP profiling was focused on the TJPs that are highly expressed in the brain, which included select claudins associated in barrier formation. Claudins have a family of 24 closely related proteins, which are subcategorized as barrier-forming claudins and pore-associated claudins [41]. In H9-NSCs, the TJP-related gene expression was identified in addition to the following pattern of expression (from high to low): claudin-3 > occludin > claudin-1 > claudin-5 > ZO-1 > claudin-12. In the case of F-NSCs, the cells showed a slightly different pattern of expression: claudin-5 > occludin > ZO-1 > claudin-

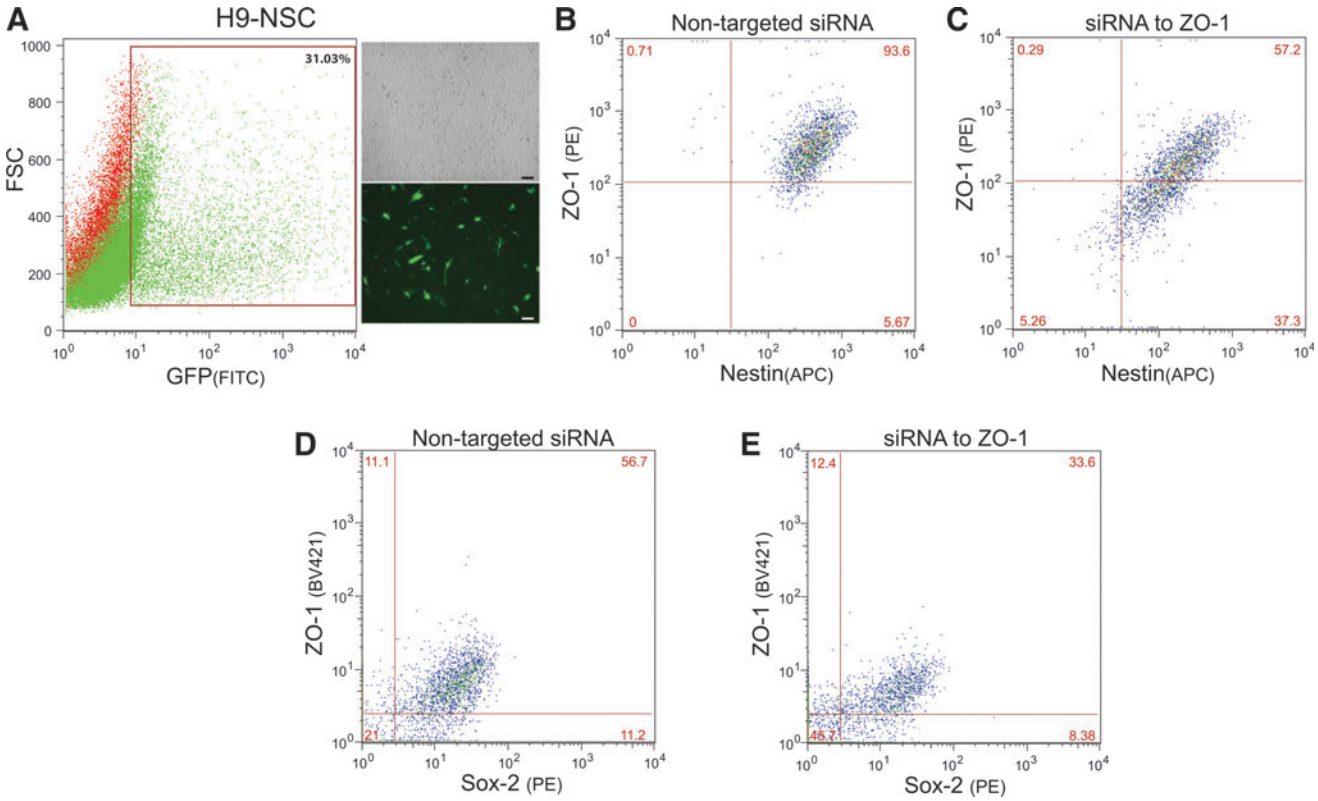

FIG. 7. siRNA-mediated knockdown of ZO-1 induces less expression of the stem cell marker, Nestin. **(A)** Indicates the transfection efficiency of H9-NSCs (microscopy images on the *right*, 10× objective magnification, scalebars at 50 μm) transfected with pooled siRNAs to TJP, ZO-1, together with a siGLO transfection indicator; a FAM-labeled oligonucleotide duplex that localizes to the nucleus. The transfection indicator was used to gate for the transfected cells and a representative graph of the gated population is indicated by the *boxed area*. **(B, D)** Representative FACS of immunolabeled ZO-1 and Nestin **(B)** or ZO-1 and Sox2 **(D)** on H9-NSCs transfected with control nontargeting siRNA. **(C, E)** Shows FACS analysis of H9-NSCs transfected with siRNAs to ZO-1 and immunolabeled for ZO-1 and Nestin **(C)** or ZO-1 and Sox2 **(E)**. Specific knockdown of ZO-1 shows a decrease in the expression of both the TJP and the stem cell markers, Nestin and Sox2. Of note, due to the use of different antibody clones for the BV421 fluorescently tagged ZO-1 and PE fluorescently tagged Sox2, the percent of cells expressing baseline levels of ZO-1 and Sox2 is lower than the more sensitive antibody clones used in Fig. 2.

1 > claudin-3 > claudin-12. Interestingly, in both types of NSCs, claudin-12 expression was marginal and ZO-2 expression was nearly undetectable. Therefore, these proteins were excluded from further analysis.

The mRNA expression was followed with validation of protein expression to determine whether the mRNA for a given TJP is stable and translated (Fig. 2). Also, given the heterogeneity of NSCs, FACS analysis allowed for measuring the percentage of cells expressing the target TJP. These analyses showed high protein expression and a high number of H9-NSCs expressing TJPs in the following order: ZO-1 > claudin-3 > occludin > claudin-5 > claudin-1. In F-NSCs, the following pattern was noted for the percent of cells expressing the subsequently given TJP (from high to low): occludin > ZO-1 > claudin-5 > claudin-3 > claudin-1. The differences in relative expression patterns of mRNA compared to protein may be explained by the possibility that changes in mRNA stability and degree of protein turnover differs for the specific TJP [32].

Although both the TJP gene and protein expression were confirmed, cellular distribution of each protein may differ to that what would be expected. Therefore, using confocal imaging, NSCs were evaluated for TJP cellular localization (ie, membranous, cytosolic, etc.) (Figs. 3 and 4). H9-NSCs had the characteristic membranous immunostaining for most of the TJP, except for claudin-5, which appeared more perinuclear and membranous. Although ZO-1 is a cytosolic protein, its close association to the membrane makes it appear membrane bound. High-magnification images for H9-NSCs (Supplementary Fig. S1) reveal an intermittent pattern for ZO-1 and a more continuous one for occludin. Therefore, it is possible that unlike barrier-forming cells, such as BMVECs, expression of TJP in NSCs provide anchoring points for cell to cell attachment. NSC neurospheres had the expected cellular distribution for all the TJPs tested. Therefore, the expression of TJPs in NSCs may be indicative of functional tight junction complexes formed at the interface between neighboring cells.

Supporting the notion that tight junction complexes are being formed can be found in results obtained from the measurement of transcellular resistance (Supplementary Fig. S2). As expected, brain endothelial cells, which are barrier forming due to the presence of tight junctions, had the highest resistance measurements (in ohms) followed by

H9-NSCs and finally HEK293 cells (which do not form tight junctions). The H9-NSCs resistance was approximately seven times higher than that measured for HEK293 cells, thus providing compelling support for the formation of tight junctions. However, the findings also reveal that the level of tight junctions present is not comparable to barrier-forming endothelial cells.

These differences between the BMVECs and H9-NSCs could simply be due to context and cytoarchitectural arrangement. BMVECs, for instance, express TJPs for assembly of a complex and highly dynamic barrier, which in vivo gives rise to the BBB. Alternatively, the expression of TJPs in H9-NSCs could likely be utilized for enhanced cell to cell attachment/anchoring. The detection of TJP expression along with an elevated transcellular resistance profile provides strong evidence that NSCs form functioning intercellular tight junction complexes.

We next hypothesized that TJPs may be inversely proportional to NSC differentiation. Thus, we examined TJP expression after induced neuronal differentiation of NSCs. We found that at 14 days of neuronal differentiation, claudin-5 and occludin expression decreased in H9 and F-NSCs (Fig. 5). Assessment of mRNA expression of all TJPs was markedly decreased at 14-day differentiation when compared to the undifferentiated state (as indicated in Fig. 6).

The above observation prompted experiments that ask the question of whether the directed elimination or decreased expression of a TJP affected the stemness status of the NSC. For this analysis ZO-1 was chosen to be targeted for siRNA-mediated knockdown due to its importance in nucleating the tight junction complex. In addition, previously it was reported that decreased expression of ZO-1 not only destabilized the TJ complex but also affected the levels of other TJPs [42]. Indeed, the H9-NSC population, in which ZO-1 was knocked down, the expression of Nestin and Sox2 was also decreased (Fig. 7). Therefore, it is possible that the decrease in TJP expression may function as a trigger for differentiation. How differentiation is affected, particularly in terms of whether TJP reduction directs the differentiation of a particular lineage, is an important future direction for this study.

Recent studies have revealed that NSCs express the gap junctional protein Cx43 both in vitro and in vivo [19,20,24,43]. Cx43 expression maintains NSCs in a proliferative state; when Cx43 expression is inhibited, NSCs differentiate or die [20,43]. In this study, we provide compelling evidence that TJPs are also present in NSCs, which together with gap junctions may (1) stabilize the intercellular arrangement and (2) promote their stem cell nature.

Previous studies have shown that NSCs exist in the specialized stem cell niches in the SVZ and SGZ of the adult mammalian brain. NSCs are in close proximity to blood vessels by which small molecules in the blood regulate NSC regeneration [3,40]. The finding in this report demonstrating the presence of TJPs in NSCs raises the possibility that NSCs may also use TJPs to aid in anchoring them to the endothelium. There is no doubt that NSCs and endothelial cells have a unique reciprocal relationship in the brain, although how BMVECs and NSCs interact to form the vascular niche is still unknown.

Interestingly, in coculture studies of BMVECs and embryonic NPCs, BMVECs increased BBB tightness, while NSCs showed suppressed differentiation [44]. Furthermore, coculture experiments have also demonstrated that NSC proliferation was induced upon removal of brain endothelial cells [45]. Unlike the above Boyden chamber studies, a recent report showed the successful direct coculture of NSCs and BMVECs together, thus demonstrating that direct interaction between the two cell types is possible [46]. Therefore, intercellular communication possibly through direct interaction of brain endothelial cells with NSCs in vascular niches may be essential for NSC self-renewal, proliferation, and differentiation.

Understanding the interactions between NSCs and the protein complexes that facilitate their cluster-like formation may provide significant insight toward understanding how these cells regulate proliferation and maintain their stemness status. Our study identifies key TJPs that are expressed on human NSCs and establishes the possibility that TJP regulation is linked to neuronal differentiation. Future studies will identify whether NSCs in neurogenic areas express TJPs, which may be essential not only in cluster formation but to also anchor NSCs to the microvasculature. Finally, how the specific TJP is temporally regulated during the three (neuronal, astrocytic, and oligodendrocyte) differentiation pathways would offer great comprehension into improving or monitoring directed differentiation of NSCs in vitro.

Acknowledgments

This study was supported (in part) by research funding from the NIH: 1R01NS086570 (to S.H.R.) and the Shriners Hospitals for Children: 85110-PHI-14 (to S.H.R.), RO1MH65151, RO1AA015913 (to Y.P.), and R01DA031064 (R.P.). The authors would like to express their appreciation to Holly Dykstra and Nancy Reichenbach for their technical support.

Author Disclosure Statement

No competing financial interests exist.

References

1. Altman J and GD Das. (1965). Autoradiographic and histological evidence of postnatal hippocampal neurogenesis in rats. J Comp Neurol 124:319–335.
2. Palmer TD, AR Willhoite and FH Gage. (2000). Vascular niche for adult hippocampal neurogenesis. J Comp Neurol 425:479–494.
3. Tavazoie M, L Van der Veken, V Silva-Vargas, M Louissaint, L Colonna, B Zaidi, JM Garcia-Verdugo and F Doetsch. (2008). A specialized vascular niche for adult neural stem cells. Cell Stem Cell 3:279–288.
4. Shen Q, Y Wang, E Kokovay, G Lin, SM Chuang, SK Goderie, B Roysam and S Temple. (2008). Adult SVZ stem cells lie in a vascular niche: a quantitative analysis of niche cell-cell interactions. Cell Stem Cell 3:289–300.
5. Yang XT, YY Bi and DF Feng. (2011). From the vascular microenvironment to neurogenesis. Brain Res Bull 84: 1–7.
6. Doetsch F and R Hen. (2005). Young and excitable: the function of new neurons in the adult mammalian brain. Curr Opin Neurobiol 15:121–128.

7. Emsley JG and T Hagg. (2003). Alpha6beta1 integrin directs migration of neuronal precursors in adult mouse forebrain. Exp Neurol 183:273–285.
8. Lu J, LC Delli-Bovi, J Hecht, R Folkerth and VL Sheen. (2011). Generation of neural stem cells from discarded human fetal cortical tissue. J Vis Exp pii:2681.
9. Deleyrolle LP and BA Reynolds. (2009). Isolation, expansion, and differentiation of adult mammalian neural stem and progenitor cells using the neurosphere assay. Methods Mol Biol 549:91–101.
10. Kanemura Y, H Mori, S Kobayashi, O Islam, E Kodama, A Yamamoto, Y Nakanishi, N Arita, M Yamasaki, et al. (2002). Evaluation of in vitro proliferative activity of human fetal neural stem/progenitor cells using indirect measurements of viable cells based on cellular metabolic activity. J Neurosci Res 69:869–879.
11. Reynolds BA and S Weiss. (1992). Generation of neurons and astrocytes from isolated cells of the adult mammalian central nervous system. Science 255:1707–1710.
12. Campos LS. (2004). Neurospheres: insights into neural stem cell biology. J Neurosci Res 78:761–769.
13. Vangipuram SD, WE Grever, GC Parker and WD Lyman. (2008). Ethanol increases fetal human neurosphere size and alters adhesion molecule gene expression. Alcohol Clin Exp Res 32:339–347.
14. Nag S, A Kapadia and DJ Stewart. (2011). Review: molecular pathogenesis of blood-brain barrier breakdown in acute brain injury. Neuropathol Appl Neurobiol 37:3–23.
15. Persidsky Y, SH Ramirez, J Haorah and GD Kanmogne. (2006). Blood-brain barrier: structural components and function under physiologic and pathologic conditions. J Neuroimmune Pharmacol 1:223–236.
16. Liu WY, ZB Wang, LC Zhang, X Wei and L Li. (2012). Tight junction in blood-brain barrier: an overview of structure, regulation, and regulator substances. CNS Neurosci Ther 18:609–615.
17. Huber JD, RD Egleton and TP Davis. (2001). Molecular physiology and pathophysiology of tight junctions in the blood-brain barrier. Trends Neurosci 24:719–725.
18. Feldman GJ, JM Mullin and MP Ryan. (2005). Occludin: structure, function and regulation. Adv Drug Deliv Rev 57:883–917.
19. Matsuuchi L and CC Naus. (2013). Gap junction proteins on the move: connexins, the cytoskeleton and migration. Biochim Biophys Acta 1828:94–108.
20. Rinaldi F, EM Hartfield, LA Crompton, JL Badger, CP Glover, CM Kelly, AE Rosser, JB Uney and MA Caldwell. (2014). Cross-regulation of connexin43 and beta-catenin influences differentiation of human neural progenitor cells. Cell Death Dis 5:e1017.
21. Sohl G, S Maxeiner and K Willecke. (2005). Expression and functions of neuronal gap junctions. Nat Rev Neurosci 6:191–200.
22. Yeager M and AL Harris. (2007). Gap junction channel structure in the early 21st century: facts and fantasies. Curr Opin Cell Biol 19:521–528.
23. Malmersjo S, P Rebellato, E Smedler, H Planert, S Kanatani, I Liste, E Nanou, H Sunner, S Abdelhady, et al. (2013). Neural progenitors organize in small-world networks to promote cell proliferation. Proc Natl Acad Sci U S A 110:E1524–E1532.
24. Cina C, JF Bechberger, MA Ozog and CC Naus. (2007). Expression of connexins in embryonic mouse neocortical development. J Comp Neurol 504:298–313.
25. Nadarajah B, AM Jones, WH Evans and JG Parnavelas. (1997). Differential expression of connexins during neocortical development and neuronal circuit formation. J Neurosci 17:3096–3111.
26. Elias LA and AR Kriegstein. (2008). Gap junctions: multifaceted regulators of embryonic cortical development. Trends Neurosci 31:243–250.
27. Kunze A, MR Congreso, C Hartmann, A Wallraff-Beck, K Huttmann, P Bedner, R Requardt, G Seifert, C Redecker, et al. (2009). Connexin expression by radial glia-like cells is required for neurogenesis in the adult dentate gyrus. Proc Natl Acad Sci U S A 106:11336–11341.
28. Peng H, Y Huang, J Rose, D Erichsen, S Herek, N Fujii, H Tamamura and J Zheng. (2004). Stromal cell-derived factor 1-mediated CXCR4 signaling in rat and human cortical neural progenitor cells. J Neurosci Res 76:35–50.
29. Koren HS, SJ Anderson and JW Larrick. (1979). In vitro activation of a human macrophage-like cell line. Nature 279:328–331.
30. Gunzel D and AS Yu. (2013). Claudins and the modulation of tight junction permeability. Physiol Rev 93:525–569.
31. Abbott NJ, L Ronnback and E Hansson. (2006). Astrocyte-endothelial interactions at the blood-brain barrier. Nat Rev Neurosci 7:41–53.
32. Ramirez SH, S Fan, H Dykstra, S Rom, A Mercer, NL Reichenbach, L Gofman and Y Persidsky. (2013). Inhibition of glycogen synthase kinase 3beta promotes tight junction stability in brain endothelial cells by half-life extension of occludin and claudin-5. PLoS One 8: e55972.
33. Bernas MJ, FL Cardoso, SK Daley, ME Weinand, AR Campos, AJ Ferreira, JB Hoying, MH Witte, D Brites, et al. (2010). Establishment of primary cultures of human brain microvascular endothelial cells to provide an in vitro cellular model of the blood-brain barrier. Nat Protoc 5:1265–1272.
34. Amasheh S, T Schmidt, M Mahn, P Florian, J Mankertz, S Tavalali, AH Gitter, JD Schulzke and M Fromm. (2005). Contribution of claudin-5 to barrier properties in tight junctions of epithelial cells. Cell Tissue Res 321: 89–96.
35. Fujita H, K Sugimoto, S Inatomi, T Maeda, M Osanai, Y Uchiyama, Y Yamamoto, T Wada, T Kojima, et al. (2008). Tight junction proteins claudin-2 and -12 are critical for vitamin D-dependent Ca2+absorption between enterocytes. Mol Biol Cell 19:1912–1921.
36. Suzuki T, S Tanabe and H Hara. (2011). Kaempferol enhances intestinal barrier function through the cytoskeletal association and expression of tight junction proteins in Caco-2 cells. J Nutr 141:87–94.
37. Nico B and D Ribatti. (2012). Morphofunctional aspects of the blood-brain barrier. Curr Drug Metab 13:50–60.
38. Ek CJ, KM Dziegielewska, MD Habgood and NR Saunders. (2012). Barriers in the developing brain and neurotoxicology. Neurotoxicology 33:586–604.
39. Pottiez G, C Flahaut, R Cecchelli and Y Karamanos. (2009). Understanding the blood-brain barrier using gene and protein expression profiling technologies. Brain Res Rev 62:83–98.
40. Gomez-Gaviro MV, R Lovell-Badge, F Fernandez-Aviles and E Lara-Pezzi. (2012). The vascular stem cell niche. J Cardiovasc Transl Res 5:618–630.
41. Krause G, L Winkler, SL Mueller, RF Haseloff, J Piontek and IE Blasig. (2008). Structure and function of claudins. Biochim Biophys Acta 1778:631–645.

42. Van Itallie CM, AS Fanning, A Bridges and JM Anderson. (2009). ZO-1 stabilizes the tight junction solute barrier through coupling to the perijunctional cytoskeleton. Mol Biol Cell 20:3930–3940.
43. Cheng A, H Tang, J Cai, M Zhu, X Zhang, M Rao and MP Mattson. (2004). Gap junctional communication is required to maintain mouse cortical neural progenitor cells in a proliferative state. Dev Biol 272:203–216.
44. Weidenfeller C, CN Svendsen and EV Shusta. (2007). Differentiating embryonic neural progenitor cells induce blood-brain barrier properties. J Neurochem 101:555–565.
45. Shen Q, SK Goderie, L Jin, N Karanth, Y Sun, N Abramova, P Vincent, K Pumiglia and S Temple. (2004). Endothelial cells stimulate self-renewal and expand neurogenesis of neural stem cells. Science 304:1338–1340.
46. Chou CH, JD Sinden, PO Couraud and M Modo. (2014). In vitro modeling of the neurovascular environment by co-culturing adult human brain endothelial cells with human neural stem cells. PLoS One 9:e106346.

Address correspondence to:
Dr. Servio H. Ramirez
Department of Pathology and Laboratory Medicine
Temple University School of Medicine
3500 North Broad Street
Philadelphia, PA 19140

E-mail: servio@temple.edu

Dr. Yuri Persidsky
Department of Pathology and Laboratory Medicine
Temple University School of Medicine
3401 North Broad Street
Philadelphia, PA 19140

E-mail: yuri.persidsky@tuhs.temple.edu

Received for publication October 23, 2014
Accepted after revision April 9, 2015
Prepublished on Liebert Instant Online April 19, 2015